crystals

MDPI

Article

Synthesis, Scrutiny, and Applications of Bio-Adsorbents from Cockle Shell Waste for the Adsorption of Pb and Cd in Aqueous Solution

Phakakorn Panpho [1], Naratip Vittayakorn [2] and Rattiphorn Sumang [1,*]

[1] Program of Physics, Faculty of Science and Technology, Pibulsongkram Rajabhat University, Phitsanulok 65000, Thailand; phakakorn.p@psru.ac.th
[2] Advanced Materials Research Unit, Department of Chemistry, Faculty of Science, King Mongkut's Institute of Technology Ladkrabang, Bangkok 10520, Thailand
* Correspondence: rattiphorn_11@hotmail.com

Abstract: Heavy metals in wastewater represent one of the most serious concerns around the world. They cause significant harm to human health. Cockle shells have been considered a source of calcium carbonate ($CaCO_3$), but their shells are disposed of as waste that pollutes the coastal environment. $CaCO_3$ has attracted considerable attention as an adsorbent for heavy metals. To ensure the meaningful use of cockle shell (CS) waste and achieve a zero-waste production system, in this study, $CaCO_3$ powder was synthesized from CS. It was characterized using XRD, TA/DTA, FESEM, and AAS. The XRD results illustrated that partial phase changes occur from aragonite (natural shell) to calcite ($CaCO_3$), calcium hydroxide ($Ca(OH)_2$), and calcium oxide (CaO) during heating. The calcined CS presented excellent adsorption performance for Pb and Cd. The Pb removal efficiency scores were about 97%, 96%, and 99% and the Cd removal efficiency scores were 100%, 98%, and 99% in a shorter time for calcined CS at 700 °C, 900 °C, and 950 °C, respectively. The results of this study show that the calcium carbonate from CS is an effective and low-cost adsorbent for the adsorption of Pb and Cd in aqueous solution.

Keywords: calcium carbonate; bio-adsorbent; cockle shells; absorbent; heavy metals

Citation: Panpho, P.; Vittayakorn, N.; Sumang, R. Synthesis, Scrutiny, and Applications of Bio-Adsorbents from Cockle Shell Waste for the Adsorption of Pb and Cd in Aqueous Solution. *Crystals* **2023**, *13*, 552. https://doi.org/10.3390/cryst13040552

Academic Editor: Michele Iafisco

Received: 5 March 2023
Revised: 18 March 2023
Accepted: 21 March 2023
Published: 23 March 2023

1. Introduction

The world is dealing with the bioaccumulation of heavy metals in the environment, which is having an immediate impact on human health and the ecosystem's food chain due to their toxicity. Therefore, it has become a primary global concern [1,2]. Heavy metals are emitted into the environment from various sources, such as the acceleration of industrialization, mining, smelting treatment, pesticide and fertilizer usage, and human activities [2–4]. Heavy metals in the form of free ions are highly toxic and carcinogenic, and their intake causes diseases and disorders since they are non-biodegradable [5,6]. Some of the harmful heavy metal ions at relatively low concentrations, such as cadmium (Cd), mercury (Hg), lead (Pb), chromium (Cr), silver (Ag), and arsenic (As), pose a potentially dangerous threat to human health, causing acute and chronic toxicities [6,7]. These heavy metal ions migrate easily within the water and remain in the environment, which can affect the quality of the water supply.

Hence, the development of an efficient technique to remove heavy metal ions from water systems is urgently required. Conventional methods for removing heavy metal ions from water and polluted aquatic environments include chemical precipitation, ion exchange, membrane methods, and electrochemical treatments. Nevertheless, there are limitations in terms of low removal efficiency, expensive equipment, and involvement with sludge production which creates treatment problems [8]. Therefore, a low-cost and environmentally friendly adsorbent is needed. Cockle is one of the most popular shellfish

products in Thailand, with an overall production total of 5200 thousand tons. The volume of shells outweighs that of shellfish by more than 70%, so it is estimated that the amount of waste shells is at least 370 thousand tons annually [9]. They are dumped into coastal areas, causing potential environmental problems. CS can be considered a cheap source of $CaCO_3$. They are made up of $CaCO_3$, mainly in the mineral form of calcite or aragonite [10,11]. $CaCO_3$ has attracted considerable attention as an adsorbent heavy metal [12]. $CaCO_3$ is a key factor for absorbents because this biomaterial can be regenerated by low-cost HCl to desorb the heavy ions and maintain high adsorption capacities after multiple cycles [13]. Using CS as an adsorbent could represent an economic and environmental way forward, as the process is highly efficient and uses low-cost materials for the exploitation of aquaculture's waste products to achieve a zero-waste production system. Many studies have used $CaCO_3$ from shellfish to absorb heavy metals in wastewater [14–16]. Following calcination treatment above 700 °C, $CaCO_3$ obtained from shells is transformed to CaO, and has been used in many applications, including as a renewable catalyst for biodiesel production [17], as a material to absorb CO_2 for air-cleaning applications [18,19], and as an initial substrate to produce hydroxyapatite ceramic biomaterials [20]. However, the transformation of $CaCO_3$ to calcium oxide (CaO) as a result of increasing calcination temperature has an impact on the absorption properties of heavy metals, as explored in a few studies. Therefore, the aim of this work is to study the influence of uncalcined and calcined shells on the phase transformations of $CaCO_3$ and on the adsorption efficiency of heavy metals in water.

2. Materials and Methods

2.1. Cockle Shell (CS) Powder Preparation

The waste CS was collected from a local supermarket. After being transported to the laboratory, the waste shells were scrubbed and cleaned thoroughly using a cellulose sponge to remove dirt. To eliminate any connective tissue and contaminated protein, the cockle shells were boiled with sodium hydroxide (NaOH) for 1 h. Then, the cleaned cockle shells were dried in an oven (Binder FED 400, GmbH Co, Germany) for 5–7 days at 80 °C. After that, the shells were crushed using a pestle and mortar (90 mm diameter Agate Top) and ground into powder. The shell powder was then sieved using a stainless-steel sieve with micro mesh (100 µm Retsch test sieve, Germany) and dried for 15 h in the oven. The shell powder was calcined at 700 °C, 750 °C, 800 °C, 850 °C, 900 °C, and 950 °C in an air atmosphere with a heating rate of 5 °C/min for 3 h and kept in an airtight polyethylene plastic bag (JP Packaging) until used to avoid a reaction with carbon dioxide (CO_2) and humidity in the air. Figure 1 summarizes the $CaCO_3$ preparation from the cockle shell and the testing method that was conducted for the X-ray diffraction (XRD) test, the microstructure test using a field emission scanning electron microscope (FESEM), and the heavy metal adsorption experiment.

2.2. CS powder Characterization

2.2.1. Thermogravimetric Analysis (TG) and Differential Thermal Analysis (DTA)

Thermogravimetric and differential thermal analyses were performed on the uncalcined (natural) CS powder from the waste cockle shell to understand the weight loss and thermal behavior of natural cockle shell powders. They were carried out using a simultaneous thermal analyzer (NETZSCH STA 449 F3 Jupiter, NETZSCH, Gerätebau GmbH, Germany) at a heating rate of 20 °C/min in an inert (Nitrogen) atmosphere in the temperature range of 30 °C–1100 °C.

2.2.2. The X-ray Diffraction (XRD) and Rietveld Refinement Characterization

To identify the crystal structure and phase of uncalcined and calcined CS powder, the X-ray diffraction (XRD) characterization was performed on an X-ray diffractometer (XRD, Philip PW 3040/60 X'Pert Pro, Eindhoven, Netherlands) using Cu Kα radiation over a 2θ

range from 10° to 80° with a step size of 0.04° at a scanning speed of 3 °/min. The XRD data were fitted with the Rietveld refinement procedure by employing the FullProf program.

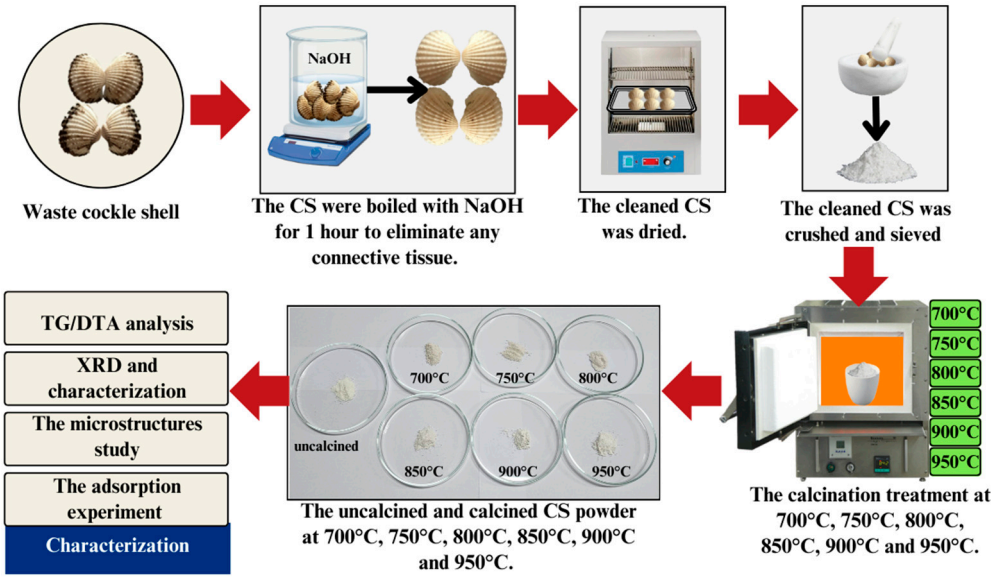

Figure 1. Schematic representation of the experimental approach.

2.2.3. The Microstructures Study

The uncalcined and calcined CS powder's microstructures were observed using a field emission scanning electron microscope (FESEM) (FESEM Apreo S, Thermo Fisher Scientific Inc., Waltham, MA, USA). The calcined shell powder was mounted on a metal stub using a silver tape-style adhesive which increases conductivity. The microscope operated at 10 kV in high-vacuum (HV) mode with an ETD detector beam current set to 0.05 nA. The FESEM morphological examination at 3000 magnification was analyzed.

2.2.4. Determination of Lead (Pb) and Cadmium (Cd) Absorption

The Pb and Cd adsorption experiments were studied as a function of the contact time by varying contact time while keeping other parameters (pH, adsorbent dose, initial concentration, and agitation speed) constant. The adsorption experiments have been presented in detail in a previous study [21]. The adsorption experiments were conducted by varying the contact time from 5 to 100 min at pH 6.0, with initial Pb and Cd concentrations of 3 mg/L. The Cd and Pb solutions were tested separately with an adsorbent dose of 1 g/L. All experiments were run in 100 mL Erlenmeyer flasks at a 200 rpm speed and at room temperature. The mixture was filtered through filter paper and the Pb and Cd concentrations in the supernatant were analyzed by atomic absorption spectrophotometry (AAS) (Perkin Elmer: PinAAcle 900F AA spectrometer, USA). The percentage removal efficiency (%E) was determined as follows:

$$\%E = \frac{(C_i - C_e)}{C_i} \times 100 \quad (1)$$

where C_i and C_e are the initial and equilibrium concentrations of Pb and Cd (mg/L), respectively [5,21].

2.2.5. Statistical Analysis

Statistical analysis was performed using OriginPro version 9 (OriginLab, Northampton, MA, USA). All the experiments were carried out in triplicate and all data are presented as mean values ± standard deviation (SD). One-way ANOVA with post hoc comparisons and the Bonferroni test were used to analyze the statistical variation between uncalcined and calcined CS powder at 700 °C, 900 °C, and 950 °C.

3. Results and Discussion

3.1. The Weight Loss and Thermal Behaviors of CS Powder

TG and DTA testing were conducted for samples taken from the uncalcined (natural) powder from the waste cockle shells. The TG/DTA curve for the uncalcined CS powder is shown in Figure 2. The expected thermal behavior was clearly visible, with four distinct stages of weight loss. There was a clear difference in the TG curves. In the first stage (I), small weight loss was observed at temperatures below 200 °C. This can be ascribed to the sample's moisture content and corresponds to a broad endothermic peak in the DTA result. In the second stage (II), at temperatures between 200 °C and 550 °C, the weight of samples decreased slightly by 1–2%, which is related to the dehydration of water from the carbonate lattice and transformation of aragonite to calcite phases [22–25]. The third state (III) was observed between 550 °C and 850 °C. The weight decreased rapidly until the samples had lost 43% of their weight and were subjected to differential thermal analysis at 828.57 °C. This state is a release process of carbon dioxide (CO_2) as a result of calcium carbonate decomposing a fraction of the sample into calcium oxide [24,25]. The final state (IV) was observed at a temperature above 850 °C. The weight of the sample remained almost constant.

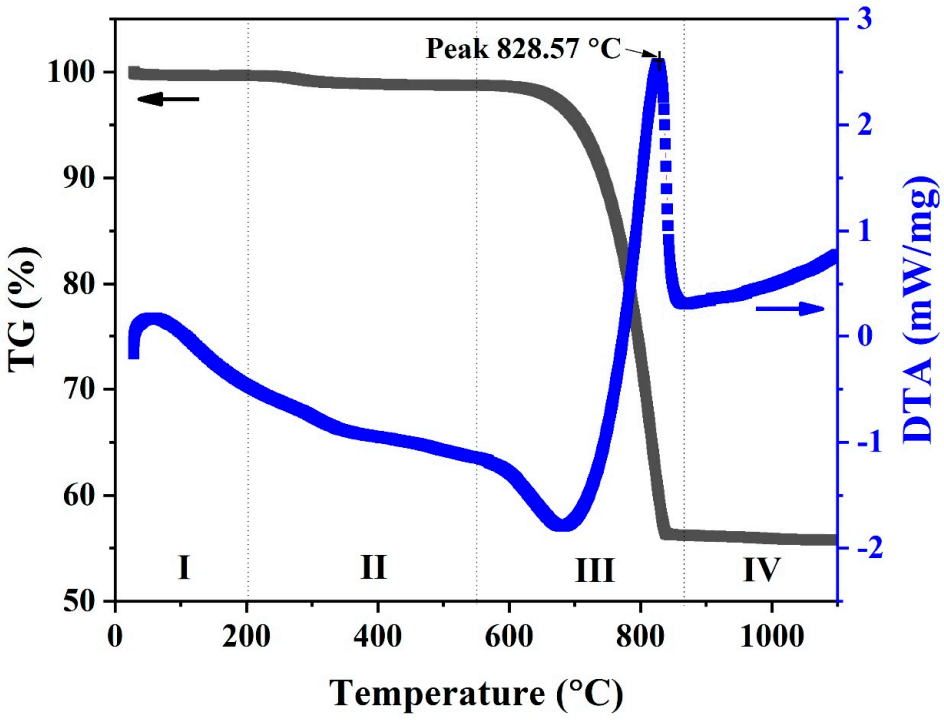

Figure 2. TG (Black line) and DTA (Blue line) curves of uncalcined (natural) powders from cockle shell.

3.2. XRD and Rietveld Refinement on X-ray Diffraction Patterns Analysis

Figure 3 shows the XRD diffraction patterns of uncalcined (natural) and calcined CS powders between 700 and 950 °C. The XRD diffraction pattern of uncalcined CS powder is characteristic of calcium carbonate in the aragonite phase (JCPDS file no. 000050453) and corresponds with previous studies [25]. XRD patterns of calcined cockle shells present a complete transformation of $CaCO_3$ to calcium oxide (CaO). At 700 °C, the samples were characteristic of calcium carbonate in the calcite phase (JCPDS file no. 010862339) as the main peak. They also presented a small peak of calcium hydroxide $Ca(OH)_2$ corresponding with JCPDS file no. 000040733. At 750 °C, the samples still contained calcium carbonate in the calcite phase of the main peak and also presented a small peak of $Ca(OH)_2$ and CaO. At 800 °C, the samples provided the main peak of CaO, corresponding to JCPDS file no. 000011160, and small peaks of $CaCO_3$ and $Ca(OH)_2$. As the calcination temperature

increased from 850 °C to 950 °C, the samples contained CaO in the main peak and a small peak of $Ca(OH)_2$. These temperatures completely removed the calcium carbonate in the calcite phase. Thus, this indicates that for the thermal decomposition of CS, $CaCO_3$ converts into CaO.

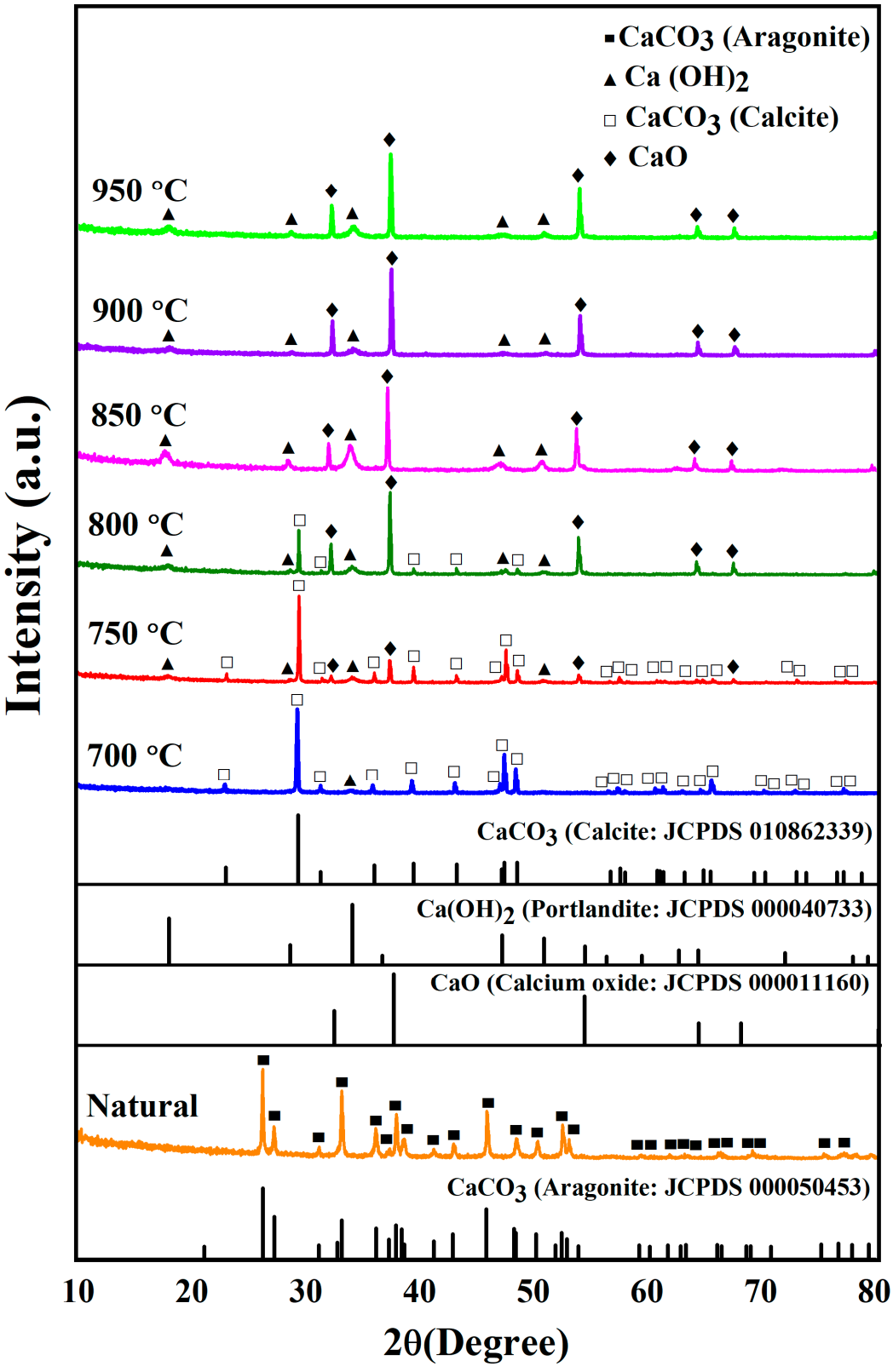

Figure 3. XRD patterns of uncalcined (natural) and calcined CS powders between 700 °C and 950 °C.

To confirm the effect of calcination temperature on the phase structure, the Rietveld refinement technique was used by fitting the XRD data with the Fullprof software, as shown in Figure 4. For simulation modeling, the cell parameter, lattice constants, space group, and atom functional positions can refer to the Crystallography Open Database (COD). In addition, the model's symmetry was changed whenever the chi-square test ($\chi 2$) and goodness of fit factor became substantially lower than in the model with a higher crystallographic symmetry [26].

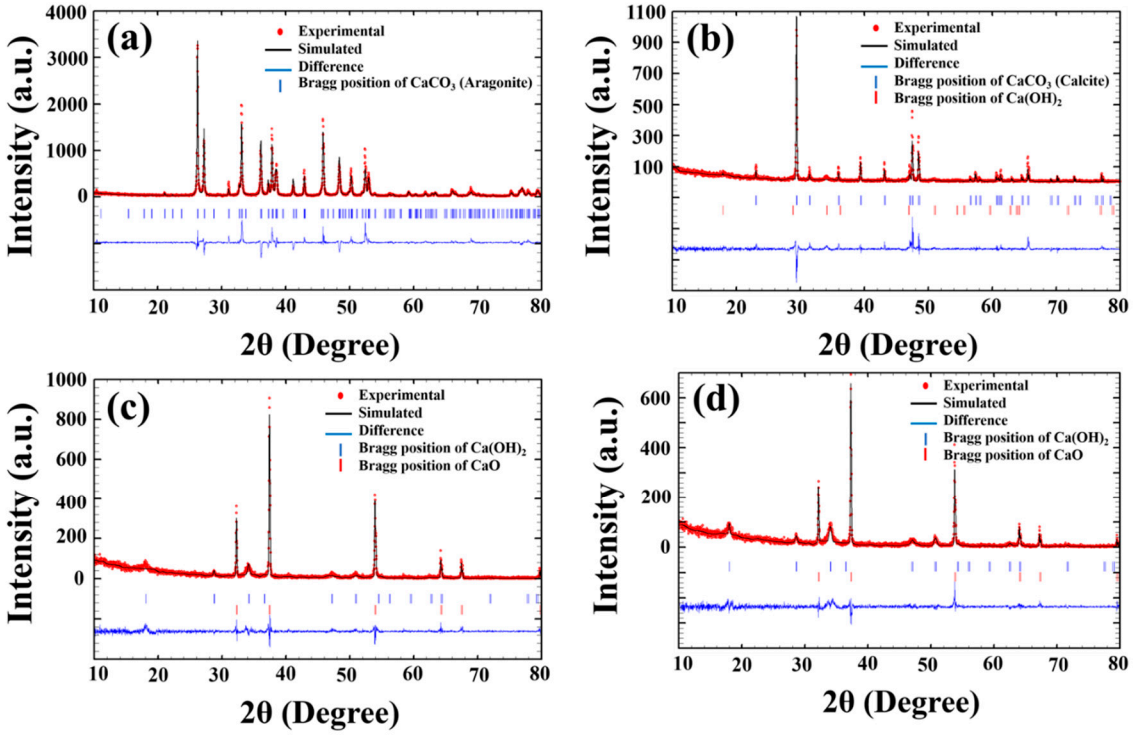

Figure 4. Fitted XRD patterns of the CS: (**a**) uncalcined and calcined CS powder at (**b**) 700 °C, (**c**) 900 °C and (**d**) 950 °C by the Rietveld refinement technique.

This result shows that there was also aragonite with space group P1 in the database for $CaCO_3$, which perfectly fits the uncalcined (natural) cockle shell powder, showing low values of χ^2 = 3.28, Rp = 24.7, Rwp = 26.6, and Rexp = 14.70, and that the phase percentage was 100%, as listed in Table 1. For the sample calcined at 700 °C, the best refinement was obtained using a mixing phase between calcite ($CaCO_3$) with space group R3C and calcium hydroxide ($Ca(OH)_2$) with space group P3m1. The phase percentages between R3C and P3m1 were 99.63 and 0.37. For the 750 °C and 800 °C samples, the triple phase of calcite ($CaCO_3$) with space group R3C, calcium hydroxide ($Ca(OH)_2$) with space group P3m1, and calcium oxide (CaO) with space group Fm3m was carried out until the best fit was obtained. The phase percentages were $CaCO_3$ = 82.50, $Ca(OH)_2$ = 7.40, and CaO = 10.10 for the samples calcined at 750 °C and $CaCO_3$ = 29.89, $Ca(OH)_2$ = 8.39, and CaO = 61.72 for the samples calcined at 800 °C. When calcination temperature increased from 850 °C to 950 °C, the P3m1 ($Ca(OH)_2$) and Fm3m (CaO) space groups were used as initial models for the refinement, which show the phase percentages of CaO = 88.15 and $Ca(OH)_2$ = 11.85 for calcination at 850 °C, CaO = 91.82 and $Ca(OH)_2$ = 8.18 for calcination at 900 °C, and CaO = 95.20 and CaO = 4.80 for calcination at 950 °C (as listed in Table 1). This indicates that calcination temperature affects the decomposition process of $CaCO_3$ from the cockle shell. $CaCO_3$ can be converted into CaO following Equation (2), which is used in industry and daily practices such as wastewater and sewage treatment, glass production, construction material, agriculture, and more [24]. CaO has also been employed as the base sorbent for carbon dioxide (CO_2) capture [27,28]. The existing materials of CO_2 adsorbents, such as

amine-based adsorbents, activated carbon, and molecular sieves, are able to withstand low-temperature processes (40 °C–160 °C) [24,27].

$$CaCO_{3(s)} \rightarrow CaO_{(s)} + CO_{2(g)} \quad (2)$$

Table 1. Rietveld structural refinement results for uncalcined (natural) and calcined CS powders between 700 °C and 950 °C.

Temp.	Goodness of Fit	Profile Parameters				The Percentage of Phase			
		$CaCO_3$ (Aragonite) (P1)	$CaCO_3$ (calcite) (R3C)	$Ca(OH)_2$ (P3m1)	CaO (Fm3m)	$CaCO_3$ (Aragonite) (P1)	$CaCO_3$ (calcite) (R3C)	$Ca(OH)_2$ (P3m1)	CaO (Fm3m)
Un-calcined	χ^2 = 3.28, Rp = 24.7, Rwp = 26.6, Rexp = 14.70	a = 4.963 Å, b = 5.748 Å, c = 7.962 Å, V = 227.181 Å^3				100			
700	χ^2 = 1.98, Rp = 68.3, Rwp = 52.9, Rexp = 37.61		a = 4.991 Å, c = 17.072 Å, V = 368.39 Å^3	a = 3.579 Å, c = 4.957 Å, V = 55.016 Å^3			99.63	0.37	
750	χ^2 = 1.84, Rp = 70.4, Rwp = 54.8, Rex = 40.37		a = 4.993 Å, c = 17.072 Å, V = 368.68 Å^3	a = 3.590 Å, c = 4.884 Å, V = 54.52 Å^3	a = 4.815 Å, V = 111.64 Å^3		82.50	7.40	10.10
800	χ^2 = 1.92, Rp = 79.5, Rwp = 58.8, Rex = 42.47		a = 4.983 Å, c = 17.113 Å, V = 368.02 Å^3	a = 3.602 Å, c = 4.880 Å, V = 54.85 Å^3	a = 4.816 Å, V = 111.27 Å^3		29.89	8.39	61.72
850	χ^2 = 1.58, Rp = 66.5, Rwp = 53.3, Rexp = 42.31			a = 3.597 Å, c = 4.919 Å, V = 55.13 Å^3	a = 4.819 Å, V = 111.93 Å^3			11.85	88.15
900	χ^2 = 1.47, Rp = 61.8, Rwp = 49.1, Rexp = 40.52			a = 3.585 Å, c = 4.907 Å, V = 54.63 Å^3	a = 4.804 Å, V = 110.92 Å^3			8.18	91.82
950	χ^2 = 1.49, Rp = 66.7, Rwp = 51.6, Rexp = 42.22			a = 3.599 Å, c = 4.923 Å, V = 55.24 Å^3	a = 4.818 Å, V = 111.84 Å^3			4.80	95.20

3.3. The Microstructures of Uncalcined and Calcined CS Powder

The surface morphologies of uncalcined and calcined CS powder at 700 °C, 900 °C, and 950 °C are listed in Figure 5. All the samples showed a non-uniform irregular with a length of up to 20 µm. The uncalcined sample showed a plate shape with parallel cleavages, as seen in Figure 5a. After calcination at 700 °C–950 °C, the surface morphologies of the sample types changed quite noticeably. The surface of calcined CS powder exhibited an agglomerated structure and a matrix phase behavior in liquid phase formation due to the removal of water and organic material from the raw shells, which is consistent with the results of Laonapakul et al. [29]. Moreover, the surface morphology increased with increasing calcination temperature, as seen in Figure 5b–d.

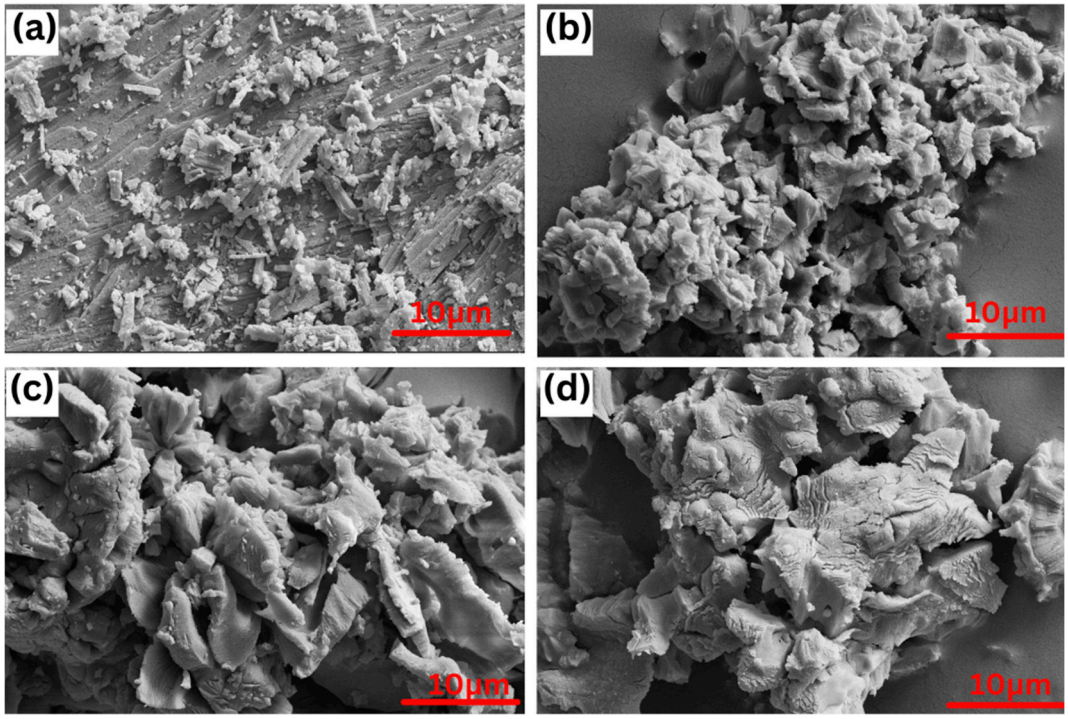

Figure 5. Representative SEM image of the CS powder: (**a**) uncalcined and calcined at (**b**) 700 °C, (**c**) 900 °C, and (**d**) 950 °C with magnification 3000.

3.4. The Pb and Cd Adsorption Capacity

The Pb and Cd adsorption levels of CS were also investigated as a function of time. Hence, the other parameters, e.g., room temperature with a 200 rpm shaking condition, the initial concentration (3 ppm), and the dosage (1 g of CS), were kept constant. Using Equation (1), the percentage removal efficiency (%E) was calculated, as illustrated in Figure 6. As shown in Figure 6a, it was observed that the Pb removal process of uncalcined and calcined CS encompasses two main stages. In the first stage, within 30 min, the Pb removal efficiency increased rapidly with an increase in the contact time. In the second stage, which took place after 30 min, the Pb removal efficiency tended to become constant. The Pb removal percentage increased over 30 min from 46.5 ± 1.4% to 91.43 ± 1.0%, 50.9 ± 0.2% to 97.6 ± 1.2%, 50.7 ± 1.2% to 96.0 ± 0.8%, and 52.5 ± 0.7% to 98.75 ± 0.7% for uncalcined and calcined CS powder at 700, 900, and 950 °C, respectively.

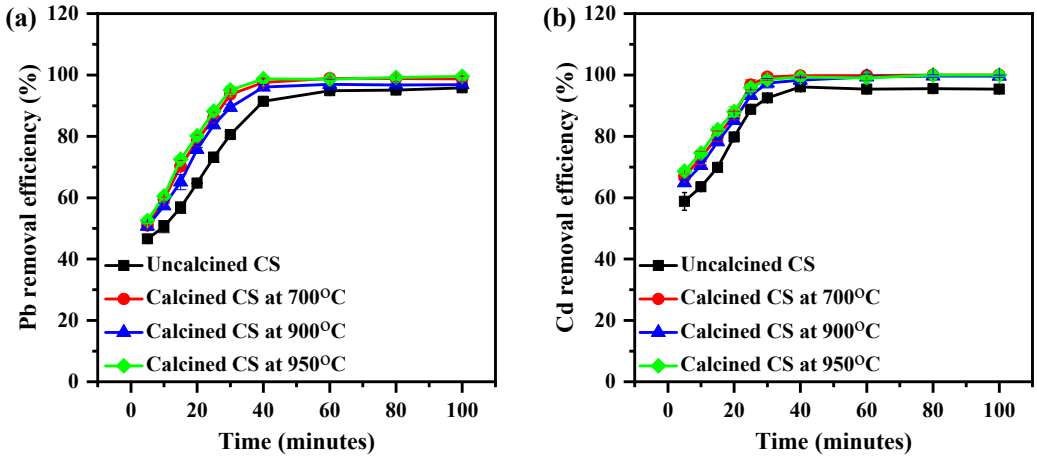

Figure 6. The effect of time on the removal efficiency of (**a**) Pb and (**b**) Cd on CS from aqueous media using the CS at various calcined temperatures (3 ppm of Cd; 1 g of CS, mixture rate of 200 rpm).

Figure 6b shows a similar trend for the Cd removal percentage of CS. It was noticed that when the time was increased from 5 to 30 min, the Cd removal rate increased from 58.8 ± 2.8% to 96.1 ± 0.5%, 66.9 ± 0.8% to 99.8 ± 0.3%, 64.8 ± 0.9% to 98.3 ± 0.7%, and 68.6 ± 0.8% to 99.3 ± 0.9% for uncalcined and calcined CS at 700, 900, and 950 °C, respectively. An explanation for this behavior is that all the sites on the surface of the calcined CS are vacant at the initial stage. However, with increasing contact time, there was a progressive increase in the number of bonds in active sites on the calcined CS surface which underwent an adsorption interaction with metal ions. The heavy metal became less efficient [30–32].

The calcination treatment's effect on the adsorption of Pb and Cd is presented in Figure 7. There were no statistically significant differences in the Pb removal efficiency when comparing the uncalcined CS at different temperatures; however, significant differences were observed between the uncalcined and calcined CS at 700 °C (p = 0.00264), (c) 900 °C (p = 0.00412), and (d) 950 °C ($p = 5.33 \times 10^{-4}$) (Figure 7a).

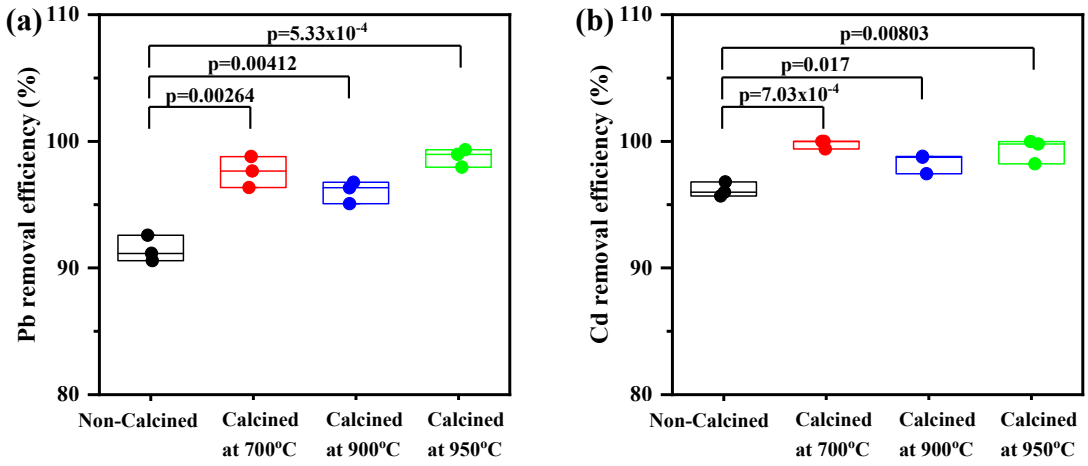

Figure 7. Box–whisker plots presented for the heavy metal removal efficiency (%) of uncalcined and calcined CS at 700, 900, and 950°C: (**a**) Pb and (**b**) Cd. All values are shown with boxes representing the 25th and 75th percentiles of data. Whiskers represent the 5th and 95th percentiles of data.

Similarly, there was a significant difference between uncalcined and calcined CS. The mean value of Cd removal percentage for uncalcined CS was lower than calcined CS at 700 °C ($p = 7.03 \times 10^{-4}$), (c) 900 °C (p = 0.0017), and (d) 950 °C (p = 0.00803) (Figure 7b). It can be explained by, as indicated in Figure 3, the XRD analysis, which showed that the crystal structure of CS is aragonite. Moreover, the surface morphology of CS presented lamellar aragonite structure before calcination, as shown in Figure 5a and as reported by Gopi et al. in 2013, who explored morphological and polymorphic transformations during the crystallization of $CaCO_3$ in the presence of DTPA [33,34]. When the CS powder was heated, the amorphous $CaCO_3$ (aragonite) was completely crystalline, and $CaCO_3$ (calcite) and CaO were found at 700 °C and 900 °C, respectively. The surface of the CS powder exhibited roughness and numerous pores appeared (Figure 5d). The phase transformation during calcination occurs as a result, and the number of small pores formed by the release of CO_2 will increase. The diffusion of Pb and Cd ions through the small pores is quick and can proceed to a larger extent [26–28].

4. Conclusions

To achieve a zero-waste production system and create wealth from waste, discarded CS was used as an effective and low-cost adsorbent for removing heavy metal ions from wastewater. Our study synthesized and investigated $CaCO_3$ from discarded CS. Based on XRD data, the characterization of discarded CS powder during calcination treatment exhibited a change in the crystal structure. Before the CS powder's calcination process,

a form of calcium carbonate was present in the CS during the aragonite phase. During heating to a calcination temperature, there was a change from $CaCO_3$ to CaO and a porous surface structure formed for the release of CO_2, as confirmed by SEM images. Therefore, the calcination temperature played a significant role in the crystal phase transformation because organic components in the CS shells can be removed to form $CaCO_3$ with pore channels on the surface, which is a critical factor for absorbents. The crystal phase transformation further affected the Pb and Cd removal percentage. The adsorption study showed that the calcined CS achieved higher adsorption performance than uncalcined CS. The Pb removal efficiency was about 97%, 96%, and 99% and the Cd removal efficiency was 100%, 98%, and 99% in a shorter time for calcined CS at 700, 900, and 950 °C, respectively. Our reported results will be helpful for understanding the crystal structure of $CaCO_3$ from CS during the calcination process for a bio-adsorption application. In addition, the high removal efficiency also supports the notion that discarded CS is a successful bio-sorbent with low cost and high effectiveness.

Author Contributions: Conceptualization, R.S., N.V. and P.P.; methodology, R.S. and P.P.; validation, R.S., N.V. and P.P.; formal analysis, R.S. and P.P.; investigation, R.S. and P.P; writing—original draft preparation, N.V.; writing—review and editing, N.V. All authors have read and agreed to the published version of the manuscript.

Funding: This research was funded by Pibulsongkram Rajabhat University, grant number RDI-2-65-24.

Institutional Review Board Statement: Not applicable.

Informed Consent Statement: Not applicable.

Data Availability Statement: The author confirms that the data supporting the reported results can be found within the article. Raw data that supports the findings of this work can be inquired to the corresponding authors, upon reasonable request.

Conflicts of Interest: The authors declare no conflict of interest.

References

1. Han, R.; Zhou, B.; Huang, Y.; Lu, X.; Li, S.; Li, N. Bibliometric overview of research trends on heavy metal health risks and impacts in 1989–2018. *J. Clean. Prod.* **2020**, *276*, 123249. [CrossRef]
2. Devi, R.V.; Nair, V.V.; Sathyamoorthy, P.; Doble, M. Mixture of $CaCO_3$ Polymorphs Serves as Best Adsorbent of Heavy Metals in Quadruple System. *J. Hazard. Toxic Radioact. Waste* **2022**, *26*, 04021043. [CrossRef]
3. Alengebawy, A.; Abdelkhalek, S.T.; Qureshi, S.R.; Wang, M.-Q. Heavy Metals and Pesticides Toxicity in Agricultural Soil and Plants: Ecological Risks and Human Health Implications. *Toxics* **2021**, *9*, 42. [CrossRef]
4. Bhunia, P. Environmental Toxicants and Hazardous Contaminants: Recent Advances in Technologies for Sustainable Development. *J. Hazardous, Toxic, Radioact. Waste* **2017**, *21*, 02017001. [CrossRef]
5. Dubey, S.P.; Gopal, K. Adsorption of chromium(VI) on low cost adsorbents derived from agricultural waste material: A comparative study. *J. Hazard. Mater.* **2007**, *145*, 465–470. [CrossRef] [PubMed]
6. Dou, D.; Wei, D.; Guan, X.; Liang, Z.; Lan, L.; Lan, X.; Liu, P.; Mo, H.; Lan, P. Adsorption of copper (II) and cadmium (II) ions by in situ doped nano-calcium carbonate high-intensity chitin hydrogels. *J. Hazard. Mater.* **2021**, *423*, 127137. [CrossRef]
7. Chakraborty, R.; Asthana, A.; Singh, A.K.; Jain, B.; Susan, A.B.H. Adsorption of heavy metal ions by various low-cost adsorbents: A review. *Int. J. Environ. Anal. Chem.* **2022**, *102*, 342–379. [CrossRef]
8. Engwa, G.A.; Ferdinand, P.U.; Nwalo, F.N.; Unachukwu, M.N. Mechanism and Health Effects of Heavy Metal Toxicity in Humans. In *Poisoning in the Modern World-New Tricks for an Old Dog?* IntechOpen: London, UK, 2019; Volume 10, pp. 77–100. [CrossRef]
9. Chalermwat, K.; Szuster, B.W.; Flaherty, M. Shellfish aquaculture in Thailand. *Aquac. Econ. Manag.* **2003**, *7*, 249–261. [CrossRef]
10. Xu, Z.; Valeo, C.; Chu, A.; Zhao, Y. The Efficacy of Whole Oyster Shells for Removing Copper, Zinc, Chromium, and Cadmium Heavy Metal Ions from Stormwater. *Sustainability* **2021**, *13*, 4184. [CrossRef]
11. Suzuki, M.; Nagasawa, H. Mollusk shell structures and their formation mechanism. *Can. J. Zool.* **2013**, *91*, 349–366. [CrossRef]
12. Zeng, C.; Hu, H.; Feng, X.; Wang, K.; Zhang, Q. Activating $CaCO_3$ to enhance lead removal from lead-zinc solution to serve as green technology for the purification of mine tailings. *Chemosphere* **2020**, *249*, 126227. [CrossRef] [PubMed]
13. Li, C.; Qian, Z.-J.; Zhou, C.; Su, W.; Hong, P.; Liu, S.; He, L.; Chen, Z.; Ji, H. Mussel-inspired synthesis of polydopamine-functionalized calcium carbonate as reusable adsorbents for heavy metal ions. *RSC Adv.* **2014**, *4*, 47848–47852. [CrossRef]
14. Lin, P.-Y.; Wu, H.-M.; Hsieh, S.-L.; Li, J.-S.; Dong, C.; Chen, C.-W.; Hsieh, S. Preparation of vaterite calcium carbonate granules from discarded oyster shells as an adsorbent for heavy metal ions removal. *Chemosphere* **2020**, *254*, 126903. [CrossRef]

15. Yavuz, Ö.; Guzel, R.; Aydin, F.; Tegin, I.; Ziyadanogullari, R. Removal of Cadmium and Lead from Aqueous Solution by Calcite. *Pol. J. Environ. Stud.* **2007**, *16*, 467–471.
16. Vu, X.H.; Nguyen, L.H.; Van, H.T.; Nguyen, D.V.; Nguyen, T.H.; Nguyen, Q.T.; Ha, L.T. Adsorption of chromium (VI) onto freshwater snail shell-derived biosorbent from aqueous solutions: Equilibrium, kinetics, and thermodynamics. *J. Chem.* **2019**, *2019*, 1–11. [CrossRef]
17. Viriya-empikul, N.; Krasae, P.; Puttasawat, B.; Yoosuk, B.; Chollacoop, N.; Faungnawakij, K. Waste shells of mollusk and egg as biodiesel production catalysts. *Bioresour. Technol.* **2010**, *101*, 3765–3767. [CrossRef]
18. Li, Y.J.; Zhao, C.S.; Chen, H.C.; Duan, L.B.; Chen, X.P. CO_2 capture behavior of shell during calcination/carbonation cycles. *Chem. Eng. Technol.* **2009**, *32*, 1176–1182. [CrossRef]
19. Ma, K.W.; Teng, H. CaO powders from oyster shells for efficient CO_2 capture in multiple carbonation cycles. *J. Am. Ceram. Soc.* **2010**, *93*, 221–227. [CrossRef]
20. Zhou, H.; Yang, M.; Zhang, M.; Hou, S.; Kong, S.; Yang, L.; Deng, L. Preparation of Chinese mystery snail shells derived hydroxyapatite with different morphology using condensed phosphate sources. *Ceram. Int.* **2016**, *42*, 16671–16676. [CrossRef]
21. Fernández Pérez, B.; Ayala Espina, J.; Fernández González, M.D.L.Á. Adsorption of Heavy Metals Ions from Mining Metallurgical Tailings Leachate Using a Shell-Based Adsorbent: Characterization, Kinetics and Isotherm Studies. *Materials* **2022**, *15*, 5315. [CrossRef]
22. Asmi, D.; Zulfia, A. Blood Cockle Shells Waste as Renewable Source for the Production of Biogenic CaCO3 and Its Characterisation. *IOP Conf. Ser. Earth Environ. Sci.* **2017**, *94*, 012049. [CrossRef]
23. Rashidi, N.A.; Mohamed, M.; Yusup, S. A study of calcination and carbonation of cockle shell. *World Acad. Eng. Technol.* **2011**, *60*, 818–823.
24. Mohamed, M.; Yusup, S.; Maitra, S. Decomposition study of calcium carbonate in cockle shell. *Eng. Sci. Technol.* **2012**, *7*, 1–10.
25. Kamba, A.S.; Ismail, M.; Ibrahim, T.A.T.; Zakaria, Z.A.B. Synthesis and Characterisation of Calcium Carbonate Aragonite Nanocrystals from Cockle Shell Powder (*Anadara granosa*). *J. Nanomater.* **2013**, *2013*, 398357. [CrossRef]
26. Gražulis, S.; Merkys, A.; Vaitkus, A.; Chateigner, D.; Lutterotti, L.; Moeck, P.; Quiros, M.; Downs, R.T.; Kaminsky, W.; Le Bail, A. Crystallography Open Database: History, Development, and Perspectives. *Mat. Inf.* **2019**, *10*, 1–39. [CrossRef]
27. Lu, H.P.; Smirniotis, G.; Ernst, F.O.; Pratsinis, S.E. Nano-structured Ca-based sorbents with high CO_2 uptake efficiency. *Chem. Eng. Sci.* **2009**, *64*, 1936–1943. [CrossRef]
28. Dennis, J.S.; Pacciani, R. The rate and extent of uptake of CO_2 by a synthetic CaO-containing sorbent. *Chem. Eng. Sci.* **2009**, *64*, 2147–2157.
29. Laonapakula, T.; Sutthia, R.; Chaikoolb, P.; Mutohc, Y.; Chindaprasirt, P. Optimum conditions for preparation of bio-calcium from blood cockle and golden apple snail shells and characterization. *Sci. Asia* **2019**, *45*, 10–20. [CrossRef]
30. Ahmadi, F.; Esmaeili, H. Chemically modified bentonite/Fe_3O_4 nanocomposite for Pb (II), Cd (II), and Ni (II) removal from synthetic wastewater. *Desalin. Water. Treat.* **2018**, *110*, 154–167. [CrossRef]
31. Heidari, B.; Bakhtiari, A.R.; Shirneshan, G. Concentrations of Cd, Cu, Pb and Zn in soft tissue of oyster (*Saccostrea cucullata*) collected from the Lengeh Port coast, Persian Gulf, Iran: A comparison with the permissible limits for public health. *Food Chem.* **2013**, *141*, 3014–3019. [CrossRef]
32. Esmaeili, H.; Tamjidi, S.; Abed, M. Removal of Cu(II), Co(II) and Pb(II) from synthetic and real wastewater using calcified Solamen Vaillanti snail shell. *Desalin. Water Treat.* **2020**, *174*, 324–335. [CrossRef]
33. Gopi, S.; Subramanian, V.K.; Palanisamy, K. Aragonite–calcite–vaterite: A temperature influenced sequential polymorphic transformation of $CaCO_3$ in the presence of DTPA. *Mater. Res. Bull.* **2013**, *48*, 1906–1912. [CrossRef]
34. Wang, Q.; Jiang, F.; Ouyang, X.K.; Yang, L.Y.; Wang, Y. Adsorption of Pb (II) from aqueous solution by mussel shell-based adsorbent: Preparation, characterization, and adsorption performance. *Materials* **2021**, *14*, 741. [CrossRef] [PubMed]